Light signals counteract alterations caused by simulated microgravity in proliferating plant cells

Aránzazu Manzano, Veronica Pereda-loth, Anne Bures, Julio Sáez-vásquez, Raúl Herranz, F. Javier Medina

Received: 23 September 2020 | Accepted: 20 April 2021

DOI: 10.1002/ajb2.1728

RESEARCH ARTICLE

Botany

Light signals counteract alterations caused by simulated microgravity in proliferating plant cells

Aránzazu Manzano[1] | Veronica Pereda-Loth[2] | Anne de Bures[3,4] | Julio Sáez-Vásquez[3,4] | Raúl Herranz[1] | F. Javier Medina[1]

[1]Centro de Investigaciones Biológicas Margarita Salas - CSIC, Ramiro de Maeztu 9, Madrid 28040, Spain

[2]GSBMS/AMIS, Université Paul Sabatier Toulouse III, Toulouse, France

[3]CNRS, Laboratoire Génome et Développement des Plantes (LGDP), UMR 5096, Perpignan 66860, France

[4]Université de Perpignan Via Domitia, LGDP, UMR 5096, Perpignan 66860, France

Correspondence

F. Javier Medina, Centro de Investigaciones Biológicas Margarita Salas - CSIC, Ramiro de Maeztu 9, Madrid 28040, Spain.
Email: fjmedina@cib.csic.es

Abstract

Premise: Light and gravity are fundamental cues for plant development. Our understanding of the effects of light stimuli on plants in space, without gravity, is key to providing conditions for plants to acclimate to the environment. Here we tested the hypothesis that the alterations caused by the absence of gravity in root meristematic cells can be counteracted by light.

Methods: Seedlings of wild-type *Arabidopsis thaliana* and two mutants of the essential nucleolar protein nucleolin (*nuc1, nuc2*) were grown in simulated microgravity, either under a white light photoperiod or under continuous darkness. Key variables of cell proliferation (cell cycle regulation), cell growth (ribosome biogenesis), and auxin transport were measured in the root meristem using in situ cellular markers and transcriptomic methods and compared with those of a 1 *g* control.

Results: The incorporation of a photoperiod regime was sufficient to attenuate or suppress the effects caused by gravitational stress at the cellular level in the root meristem. In all cases, values for variables recorded from samples receiving light stimuli in simulated microgravity were closer to values from the controls than values from samples grown in darkness. Differential sensitivities were obtained for the two nucleolin mutants.

Conclusions: Light signals may totally or partially replace gravity signals, significantly improving plant growth and development in microgravity. Despite that, molecular alterations are still compatible with the expected acclimation mechanisms, which need to be better understood. The differential sensitivity of *nuc1* and *nuc2* mutants to gravitational stress points to new strategies to produce more resilient plants to travel with humans in new extraterrestrial endeavors.

KEYWORDS

abiotic stress, auxin transport, cell cycle, graviresponse, nucleolin, ribosome biogenesis, root meristem, space plant biology

Plants live in dynamic environments, with frequent changes in many parameters, such as temperature, humidity, water and light. Since plants are sessile organisms, they have developed different directional responses to modulate their growth according to environmental cues, which are termed tropisms. The two major tropistic cues are gravity and light (Molas and Kiss, 2009). Gravitropism and phototropism drive plant growth and development by producing opposite effects in the roots and in the aerial parts of the plant. Roots grow in the opposite direction to the light source and in the direction of the gravity vector (negative phototropism and positive gravitropism), whereas the aerial parts show negative

Abbreviations: ETS, external transcribed spacer, either in the transcription unit of rRNA genes, or in pre-rRNA primary transcript; *g*, acceleration of gravity: 9.8 $m \cdot s^{-2}$; GUS, β-glucuronidase; IOD, integrated optical density; RPM, random positioning machine; RT-(q)PCR, real time-(quantitative) polymerase chain reaction; YFP, yellow fluorescent protein.

gravitropism and positive phototropism (Vandenbrink et al., 2014). The phytohormone auxin is a key factor in the transduction pathway of the tropistic response to these two signals, playing a mediating role between perception and response (Ottenschlager et al., 2003; Christie and Murphy, 2013).

Plant development, driven by tropistic cues, is supported by the activity of the meristematic tissues. These tissues are characterized by the balance between cells actively proliferating, involved in a continuous cell cycle, and the cells escaping from the cell cycle to differentiate (Scheres et al., 2002; Perrot-Rechenmann, 2010). In fact, meristems constitute the source of cells for growth and differentiation, being the cellular basis for the developmental program of the plant. Meristematic cells are undifferentiated highly proliferating cells, which maintain a strict coordination between cell proliferation and cell growth, which is termed "meristematic competence" (Mizukami, 2001).

The growth of meristematic cells is not merely an increase in size, but it depends on a continuous supply of proteins, enabling them to reach the critical size necessary for cell division. Ribosomes are the protein factories of cells, so the rate of ribosome biogenesis is directly correlated to the cell growth (Baserga, 2007; Sablowski and Carnier Dornelas, 2014). Thus, in proliferating meristematic cells, cell growth is ultimately determined by RNA polymerase I activity, which controls ribosomal RNA synthesis and ribosome biogenesis in the nucleolus (Weis et al., 2015). An unequivocal functional link between the rate of ribosome biogenesis and the nucleolar ultrastructure has been demonstrated in plants, using cellular models characterized by high cell proliferation rates (Medina et al., 2000; Sáez-Vásquez and Medina, 2008). Ribosome biogenesis is indeed a complex process integrated by multiple steps. The nucleolar protein nucleolin is the most abundant protein of exponentially growing cells and plays a major role in the regulation of ribosome biogenesis at different levels, namely, rDNA chromatin structure, rRNA gene transcription, pre-rRNA processing and export of pre-ribosomal particles, and even in the structural organization of the nucleolus (Mongelard and Bouvet, 2007; Medina et al., 2010; Durut and Sáez-Vásquez, 2015). The *Arabidopsis thaliana* genome contains two nucleolin genes, termed *NUC1* and *NUC2*. Under normal conditions, *NUC1* is expressed at a high rate, mostly in proliferating tissues (Pontvianne et al., 2007), whereas the protein NUC2 plays a role in rDNA chromatin dynamics, preferentially at developmental transitions (Durut et al., 2014). Furthermore, NUC2 is involved in the plant stress response (Durut et al., 2019).

Cell growth, ribosome biogenesis, cell proliferation, and the cell cycle, as cellular activities taking place in meristematic cells and defining meristematic competence, are primary targets of tropistic cues. In the case of light, specialized photoreceptor proteins—phytochromes—are modulators of cell proliferation and cell growth in meristems. This modulation is different for the shoot and for the root meristematic cells, in agreement with the opposite phototropic behavior of the shoot and the root. In the shoot apical meristem, light irradiation plays an activating role, promoting cell cycle progression of cells previously arrested at G1 or G2 phases in darkness (López-Juez et al., 2008; Mohammed et al., 2018). In contrast, in the root meristem, light induces the production of flavonols and other metabolites resulting in a reduction of the cell proliferation rate (Silva-Navas et al., 2016). Light also indirectly regulates cell proliferation and cell growth via photosynthesis. Sugars synthesized in the photosynthetic process play a regulatory role in meristematic tissues. Glucose binds to the central regulator TOR kinase inducing the activation of cell proliferation, through the expression of S-phase genes, and ribosome biogenesis (Caldana et al., 2013; Xiong et al., 2013; Sablowski and Carnier Dornelas, 2014).

The other major tropistic cue, gravity, also has an impact on meristematic activity. Gravity alterations induce changes in the rate of cell proliferation and cell growth in root meristematic cells, as shown in experiments under real or simulated microgravity (Matía et al., 2010; Manzano et al., 2013). These experiments were done in the dark (i.e., without any major tropistic cue) and using a culture medium supplemented with sucrose (10 g/L). In these cells, the lack of gravity appeared as a stress condition, resulting in the disruption of meristematic competence. *Arabidopsis thaliana* seedlings grown in microgravity and darkness had increased cell proliferation and decreased cell growth (Matía et al., 2010; Manzano et al., 2013). These alterations were accompanied by an inhibition of auxin polar transport in root tips (Manzano et al., 2013). The absence of gravity is a major environmental change during spaceflight, and planets and satellites other than the Earth are characterized by a different level of gravity compared to our planet. Therefore, alterations in plant development caused by changes in gravity may compromise the growth of plants for human space exploration or future human settlement on other planets. Higher plants are indeed an essential component of the life support systems that must be implemented for these purposes.

A close relationship between the regulatory effects of light and gravity on plant growth was recently found by showing that light modulates the gravitropic response by regulating the expression of *LAZY4*, a gene that plays an important role in the gravitropic response of both shoots and roots (Yang et al., 2020). The role of light is played through two classes of transcription factors: in hypocotyls, by phytochrome interacting factors (PIFs), which are negative regulators of photomorphogenesis, and in roots by elongated hypocotyl 5 (HY5), which promotes plant photomorphogenesis under diverse light conditions (Yang et al., 2020). In addition, upregulation of genes involved in a fundamental light-dependent function, such as photosynthesis, has been found as a response to the microgravity condition in spaceflight, and, interestingly, this response occurred in etiolated plants, in the absence of any light signal (Kruse et al., 2020). However, despite these findings, many other factors of the mechanism by which light and gravity crosstalk for regulating plant growth remain unclear. Consequently, the question on whether light can compensate for the deleterious effects of altered gravity remains unanswered. As indicated above, this question is critical for the success of plant culture in future human settlements on other planets.

Here, we sought to better understand the interactions between the two main tropistic signals and the combined effects of their presence or absence on the functions of meristematic cells, taking into account the fundamental role played by phototropism and gravitropism on meristematic activity and, hence, on plant development. Specifically, we aimed at discriminating whether or not light can act as a counteracting factor to reverse the effects caused by the lack of gravity orientation in darkness on the basic functions of meristematic cells, and to what extent. Therefore, the main purpose of this work is not focused on the tropistic phenomena per se, but on the developmental consequences of the interactions between the two signals triggered by their combined action on meristems. We used a random positioning machine (RPM), a reliable and well-characterized microgravity simulator (Herranz et al., 2013) and applied two illumination regimes, either photoperiod or darkness, then evaluated the status of meristematic competence (the balance between cell proliferation and cell growth) in the root of 6-day-old seedlings, that is, during the early stages of plant development. We paid special attention to ribosome biogenesis, which is fundamental to maintaining meristematic competence (Sáez-Vásquez and Medina, 2008). For this reason, we chose two mutants for nucleolar protein nucleolin, an essential factor in the regulation of ribosome biogenesis, that has a clear influence on the regulation of cell cycle (Medina et al., 2010). The *nuc1* and *nuc2* mutants do not have any visible phenotype related to gravitropism or phototropism deficiency unless they are examined at the cellular level; alterations in ribosome biogenesis are evident as modifications in the size and structure of the nucleolus, which have been thoroughly described (Pontvianne et al., 2007; Durut et al., 2014) and were used as markers in the present study. Furthermore, a differential response to simulated microgravity under two lighting regimes (darkness and photoperiod) has been described for these mutants in ground gravity in the darkness and in red light (Manzano et al., 2020). Complementary analyses were done separately in roots and hypocotyls (aerial parts) of seedlings grown to determine whether differential contributions to the effects are shown for each light and gravity condition. Our results showed that light can effectively replace gravity, at least partially, as a tropistic cue driving plant development by attenuating the effects caused by microgravity on the root meristem.

MATERIALS AND METHODS

Experimental setup and seedling growth conditions

Five commercially available lines of *Arabidopsis thaliana* were used: ecotype Columbia (wild-type Col-0, initially obtained from Lehle Seeds, Round Rock, TX, USA, then propagated in our laboratory), two mutants of the nucleolin protein gene (*nuc1.2* and *nuc2.2*) (Pontvianne et al., 2007; Durut et al., 2014) (Nottingham Arabidopsis Stock Centre *nuc1.2*: Salk_002764; *nuc2.2*: GABI178D01), a reporter line of cyclinB1 gene expression, CYCB1:*uid*A (Ferreira et al., 1994) (Nottingham Arabidopsis Stock Centre CS68143), and a reporter line of auxin distribution pattern, DII-VENUS (Brunoud et al., 2012) (Nottingham Arabidopsis Stock Centre CS799173).

Seeds were sterilized for 4 min in 70% (v/v) ethanol (Sigma, St. Louis, MO, USA #270741) and 1% (v/v) Triton X-100 (Sigma #T9284), then washed two times with 95% ethanol for 1 min each. Once dried, seeds were glued on a nitrocellulose membrane (#28149-472; VWR, Monroeville, PA, USA) with gum guar (1% w/v, Sigma #G-4129). For seedlings grown for transcriptomic analysis (to be frozen at −80°C after growth), seeds were arranged in two rows (100 seeds/row). When seedlings were grown for microscopic analysis (to be chemically fixed after growth), seeds were arranged in a single row (30 seeds/row).

Membranes containing seeds were placed on 6-cm-diameter Petri dishes containing 0.8% (w/v) agar with ½ MS (Murashige and Skoog's, Duchefa, Haarlem, Netherlands) plant culture medium, half strength, without sucrose, and stratified at 4°C for 2 days to induce rapid, synchronous germination.

Petri dishes were mounted in the random positioning machine (desktop RPM; Dutch Space, Leiden, Netherlands; located at the Université III-Paul Sabatier, Toulouse-France) (ground microgravity simulator, effective gravity $\leq 10^{-4} \times g$) (Borst and van Loon, 2009) (Appendix S1). Half of the seedlings were grown with 16 h of unidirectional white light and 8 h of darkness using White X4 Ultra Bright LED lights (#AN-D420HWA; Purdy Electronics, Mountain View, CA, USA) to provide a photosynthetic photon flux of 40 μmol m^{-2} s^{-1} at a distance of 40 mm from the top of the seedlings. The other half of the seedlings were grown in continuous darkness. Seeds germinated and seedlings grew at 22°C, with 80% relative humidity, for 6 days.

For each experiment, we performed a control at Earth gravity level (hereafter, 1 *g*). In the control condition, the plants grew in Petri dishes attached to the frame of the RPM, under the same conditions of illumination, temperature, humidity, and even vibrations, as the RPM samples.

After the growth period, the plates with 200 seeds were directly frozen at −80°C. The plates with 30 seeds were open to take images, and the seedlings were quickly recovered from the dishes and transferred within 15 min into fixative solutions. The Col-0, *nuc1*, *nuc2* and DII-VENUS plants were immersed in 5% v/v paraformaldehyde in PBS, and CYCB1:*uidA* plants were stored in cold acetone (−20°C), then processed as described next.

Sample processing for microscopic analyses

Immunofluorescence and nucleolar area quantification

The Col-0, *nuc1*, *nuc2* and DII-VENUS seedlings were fixed in 5% (v/v) paraformaldehyde in PBS, pH 7.2, for 3 h at room temperature, washed three times for 10 min each with

PBS, and incubated for 1 h at 37°C with a cell-wall-digestion solution of 2% w/v cellulase (Sigma #1794), 1% w/v pectinase (Sigma #17389), 0.05% w/v macerozyme (#28302; Serva, Heidelberg, Germany), 0.4% w/v mannitol, 10% v/v glycerol and 0.2% v/v Triton X-100. After cell-wall digestion, the seedlings were washed three times, 10 min each, with PBS supplemented with 10% (v/v) glycerol and 0.2% (v/v) Triton X-100. Excised root tips were placed on multi-well slides (EMS #63422-06) coated with poly-L-lysine (Sigma #P8920), and the samples were dehydrated with 100% methanol at –20°C for at least 30 min.

Slides were washed twice, 5 min each, with PBS, supplemented with 1% (v/v) NP40 (Sigma #D67509) and 0.5% (w/v), sodium deoxycholate (DOC; Sigma #I3021) and pre-treated with blocking buffer (2% w/v BSA and 0.05% v/v Tween in PBS) for 30 min at room temperature. Then, they were incubated overnight at 37°C (in a humidified atmosphere) with mouse monoclonal anti-fibrillarin 38F3 antibody (#ab4566; Abcam, Cambridge, UK), diluted 1:1000 in blocking buffer. Following incubation, wells were washed (3 times, 5 min each) with PBS, containing 1% v/v NP40 and 0.5% w/v DOC and incubated for 3 h at 37°C with a second antibody (anti-mouse IgG-Alexa 488, diluted 1:100) (#A11001 Invitrogen, Thermo Fisher Scientific, Waltham, MA, USA. Then, samples were washed with the same buffer, and nuclear DNA was stained with 4′6-diamidino-2-phenylindole (DAPI 5×, Thermo Fisher Scientific, Waltham, MA, USA). Finally, slides were washed with PBS and distilled water (twice, 5 min each) and mounted with DABCO (anti-fading agent; Sigma #290734). The root tips were examined and micrographs taken with a confocal laser microscope (Leica TCS SP5). Nucleolar size (area immunostained for fibrillarin) was measured using the software ImageJ (National Institutes of Health, Bethesda, MD, USA).

Cell membrane staining and cell proliferation quantification

Seedlings were fixed in 5% v/v paraformaldehyde for 3 h at room temperature, washed three times for 10 min each with PBS and incubated 1 h at 37°C with the cell-wall-digestion solution described above. After cell-wall digestion, the seedlings were washed with PBS containing 10% v/v glycerol and 0.2% v/v Triton X-100 (3 times, 10 min each), excised root tips were placed on poly-L-lysine coated multi-well slides, and the samples were dehydrated with 100% methanol at –20°C for at least 30 min.

Root tips were stained for 2 h at room temperature in darkness with dye solution: 2% v/v Renaissance (#SCRI 2200; Renchem, North Duffield, Selby, UK) + 4% v/v DMSO in PBS, pH 7.2. Then, the samples were washed with PBS and distilled water (3 times, 5 min each), and DABCO was added. Samples were observed and images taken with a confocal laser microscope (Leica TCS SP5). Finally, the number of cells/mm in root meristematic cell layers was counted using ImageJ software to determine the rate of local cell production (Beemster and Baskin, 1998). DII-VENUS fluorescence intensities were extracted from the confocal images using the CellSeT segmentation tool as described by Pound et al. (2012).

Histochemical GUS assay

Seedlings were incubated in acetone at –20°C for 3–4 days. Then, the samples were washed (twice, 10 min) with 100 mM sodium phosphate buffer, and the GUS signal was revealed by enzymatic reaction (5 mM potassium ferrocyanide and ferricyanide), 100 mM sodium phosphate buffer and 40 mM X-glucuronide CHA salt (X-Glc A, Duchefa #X1405.0100) overnight, at 37°C, in darkness.

Reactions were stopped by several washings of samples in 50 mM sodium phosphate buffer before being mounted with glycerol on 8 × 8 mm well slides. The root tips were observed under a Leica DM2500 microscope, and images were recorded with a Leica DFC320 CCD camera and processed with ImageJ software. Integrated optical density (IOD) was calculated (IOD = stained area × OD in the blue light spectrum) using an unstained zone of the root tip as the blank.

Sample processing for transcriptional analyses

RNA extraction

Frozen samples were dissected by separating aerial parts (hypocotyls) from roots, and seeds (ungerminated or remnants) were discarded for avoiding any changes of expression results. Total RNA from plant tissues (shoots and roots) was extracted with a commercial kit (RNA isolation from plant, NucleoSpin) following the manufacturer's instructions (#740949.250; Macherey-Nagel, Dueren, Germany). RNA quality was determined by NanoDrop 2000 (Thermo), and samples were stored at –80°C until further use.

Pre-rRNA processing study in hypocotyls (RT-PCR)

Extracted RNAs from aerial parts were used to analyze ribosome biogenesis, specifically pre-rRNA processing, by conventional RT-PCR with probes corresponding to different external transcribed spacer (ETS) sequences of 45 S pre-rRNA (primary transcript) (Appendix S2) (Pontvianne et al., 2010; Durut et al., 2014).

The samples (5 µg) were treated with an extra DNase digestion (TURBO DNase Treatment and Removal Reagents, #AM1907; Ambion, Waltham, MA, USA) for 60 min to eliminate contaminant DNA. First-strand cDNA synthesis was performed on 500 ng of treated RNA with the Oligo (dT)15 (#C1101; Promega, Madison, WI, USA) and Random Primers (Promega #C1181) using the SuperScript

III Reverse Transcriptase kit and the manufacturer's instructions (Invitrogen, Waltham, MA, USA #18080-093). RNA quality was checked after the DNase treatment, and a negative RT (RT-) control (without enzyme) was included.

The 5′ and 3′ETS sequences from cDNA products (PCR products) were amplified with GoTaq DNA Polymerase (Promega #M7845) and oligonucleotides 5′ETS (p1/p2), 5′ ETS-P/18 S (p3/p4), 5′ETS/18 S (p5/p6), 25 S/3′ETS (p7/p8) and 3′ETS (p9/p10) using the manufacturer's instructions. PCRs were performed in parallel in RT + and RT- samples. In addition, an extra negative control (no sample) with ddH_2O and positive control (genomic DNA, 2.9 ng/μL) were included.

PCR products (5 μL) were separated by electrophoresis in an agarose gel (2% w/v in 0.5× Tris-acetate-EDTA buffer) for 1 h at 130 V. The eIF1α transcription factor was used as a loading control and internal standard (no expression changes in any experimental condition). Images for each gel were recorded using the Kodak Electrophoresis Documentation and Analysis System 120 coupled to DC290 Zoom Digital Camera and analyzed with ImageJ.

Pre-rRNA processing and meristematic competence studies in roots (RT-qPCR)

Quantitative RT-PCR (RT-qPCR) was performed in a single step with the LightCycler 96 System (Roche, Basel, Switzerland) and Brilliant III Ultra-fast SYBR Green QRT-PCR Master Mix (Agilent Technologies, Santa Clara, CA, USA) with primers corresponding to selected genes involved in ribosome biogenesis, cell cycle regulation, cell growth, and auxin polar transport (Appendix S3). RT-qPCR was performed in standardized conditions (40 cycles and 60°C hybridization phase temperature) after testing that all probe combinations produced a single peak (amplicon) and that RNA/probe concentration ratios were in the optimal efficiency range of the qPCR reaction (Appendix S4). The *Actin2* gene was used as an internal standard, and results were analyzed using the comparative cycle threshold method relative to input (Appendix S5) (Livak and Schmittgen, 2001). Once the amount of target or $2^{-\Delta\Delta C_T}$ was obtained, to determine the number of times that each gene of interest is expressed in simulated microgravity with respect to the control condition, we calculated the ratio or fold-change by dividing these two values (Fold-change = $2^{-\Delta\Delta C_T}$ RPM/ $2^{-\Delta\Delta C_T}$ 1 at 1 *g*). This calculation was carried out independently for each of the genotypes studied. Finally, when the fold-change was a number less than 1, a transformation (–1/Fold-change) was carried out so that the changes between both experimental conditions, corresponding to different gravity levels, were easier to visualize and compare.

Statistical analyses

SPSS 22.0 software (IBM, Armonk, NY, USA) was used for all analyses. First, we checked for normal distribution (Shapiro–Wilk test for $N < 20$ or Kolmogorov–Smirnov test for $N > 20$) and homoscedasticity (Levene test).

Quantitative variables were described using mean and standard deviation values. Means were compared using Student's *t*-test for independent samples (normal distribution and homoscedasticity) or by nonparametric *U* Mann–Whitney–Wilcoxon Test (non-normal distribution). All statistical analyses were carried out by comparing, for each lighting regime, the simulated microgravity experimental condition with respect to its corresponding 1 × *g* control, in plants of the same genotype. As a general rule, differences between samples were considered significant for a bilateral probability value, *P*, lower than 0.05 ($P < 0.05$); however, a more stringent probability value ($P < 0.0125$) was also applied to reduce the chance of false positives in the four comparisons (Appendix S6). In addition, a two-way ANOVA test is provided as supplementary material (Appendix S7). This factorial variance analysis was carried out using a univariate (general linear model) procedure, defining as dependent variables each measured variable and as fixed factors (categorical independent variables) the light and the gravity.

RESULTS

Seedling growth: root and hypocotyl orientation and length

Seedlings of the Col-0, *nuc1*, and *nuc2* genotypes were grown for 6 days in vertical position (1 *g* control), either with photoperiod regime or dark conditions. Seed germination rate decreased and growth was somewhat retarded for *nuc1* mutants, which had an irregular growth rate. In all cases, the roots of seedlings were oriented in the direction of the gravity vector and opposite the light source (positive gravitropism and negative phototropism). Hypocotyls were oriented opposite to gravity and, in the case of illumination, toward the top light source (negative gravitropism and positive phototropism) (Figure 1G–L). Simulated microgravity samples with photoperiod regime presented the same orientation as 1 *g* control samples, except for a slight disorganization of the roots, while samples grown in darkness and microgravity (without any tropistic cues) showed a total disorganization in their growth (random growth) (Figures 1A–F, 2). A slight anti-gravitropic preferential direction for the roots was detected in the *nuc1* mutant and, even less pronounced, in the Col-0 wild-type, but not in the *nuc2* mutant (Figure 2). In the case of shoots, the anti-gravitropic growth was more evident in all genotypes, but the growth direction was never coincident with the vertical axis (Figure 2). A conspicuous skewing of hypocotyls in the conditions of absence of light and gravity was observed. This effect was especially relevant for the wild type (Col-0) seedlings, in which hypocotyls showed a sort of parallel alignment, and it appeared relatively attenuated in the two mutant lines (Figures 1 and 2). It is noteworthy that this

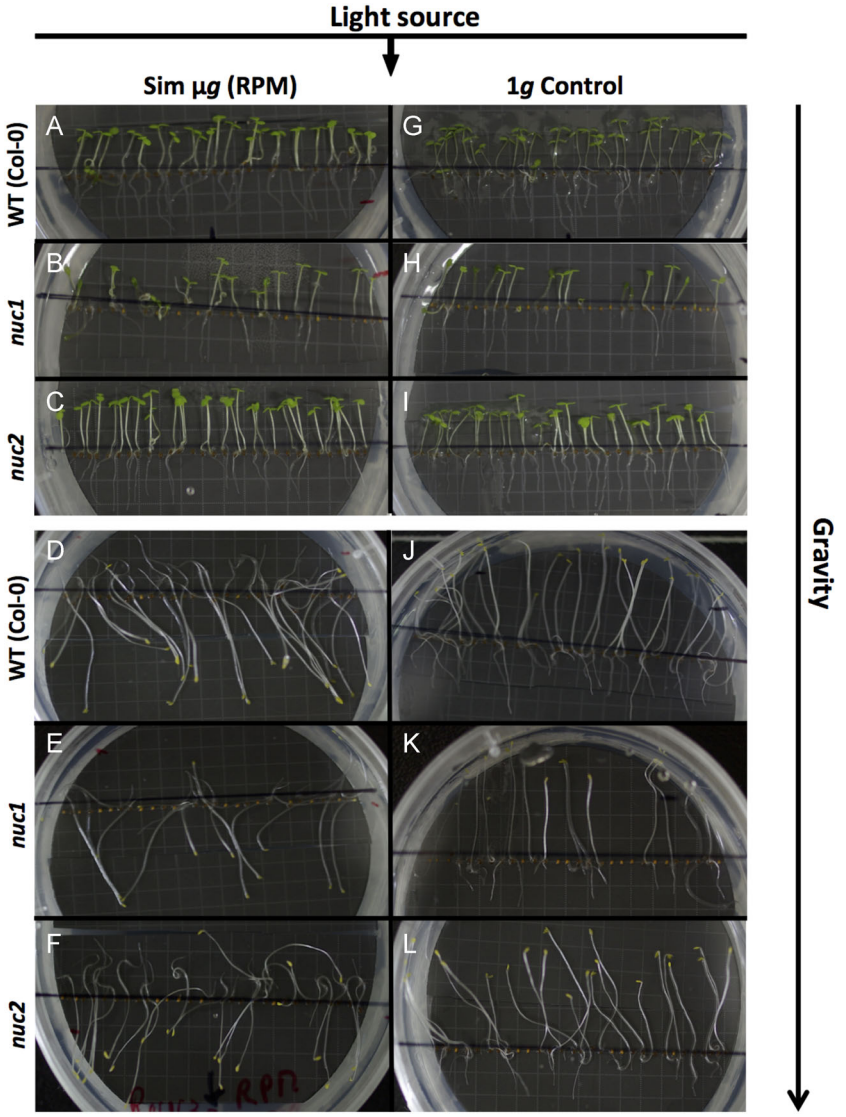

FIGURE 1 *Arabidopsis thaliana* seedlings grown under simulated microgravity (RPM) and 1*g* control conditions. Images of 6-day-old seedlings (Col-0, *nuc1* and *nuc2*) grown under simulated microgravity (A–F) either with photoperiod regime (A–C) or darkness (D–F) and their corresponding 1*g* control (G–L). Gravity vector and light source direction were indicated in the figure

skewness of hypocotyls was restricted to the conditions of microgravity and darkness and did not appear in any other condition.

Root length was shorter for all seedlings grown in darkness (except in the case of the *nuc1* mutant) (Figure 3A, C), and this variable showed a slight decrease in all samples grown in microgravity and photoperiod; this decrease was only significant with respect to the corresponding 1 *g* control in the *nuc2* mutant (Figure 3A and Appendix S6). In contrast, this variable was not affected, in comparison with control condition, in any of the lines grown in microgravity and darkness (Figure 3C).

Hypocotyls appeared clearly elongated in seedlings grown in darkness (etiolated seedlings) in all genotypes and gravity conditions (Figure 3). For seedlings grown under the photoperiod, the change in the gravity level did not produce any effect on the hypocotyl length (Figure 3B). However, in darkness, some differences appeared in the three lines, and the *nuc2* mutant had a significantly shorter hypocotyl when grown in simulated microgravity (Figure 3D; Appendix S6).

Pre-rRNA processing study

Pre-rRNA processing in the aerial part (hypocotyl)

Alterations in the ribosome biogenesis process in hypocotyls were investigated by analyzing different steps of 45 S pre-rRNA (primary transcript) processing by RT-PCR. We detected nucleotide sequences corresponding to different regions of the transcript that are cleaved at known steps of transcript processing. These sequences corresponded to 5′ETS and 3′ETS only or to 5′ETS/18 S and 25 S/3′ETS transcripts (Pontvianne et al., 2010) (Figure 4A). The analysis by RT-PCR identified potential enrichments in intermediate RNAs, which could account for changes in the accumulation of 45 S pre-rRNA and/or processed spacer sequences.

When comparing the amplified bands linked to the different steps of 45 S pre-rRNA processing, no differential patterns were observed in simulated microgravity under any light regime (photoperiod or darkness) for any *Arabidopsis thaliana* line, when they were compared to the control

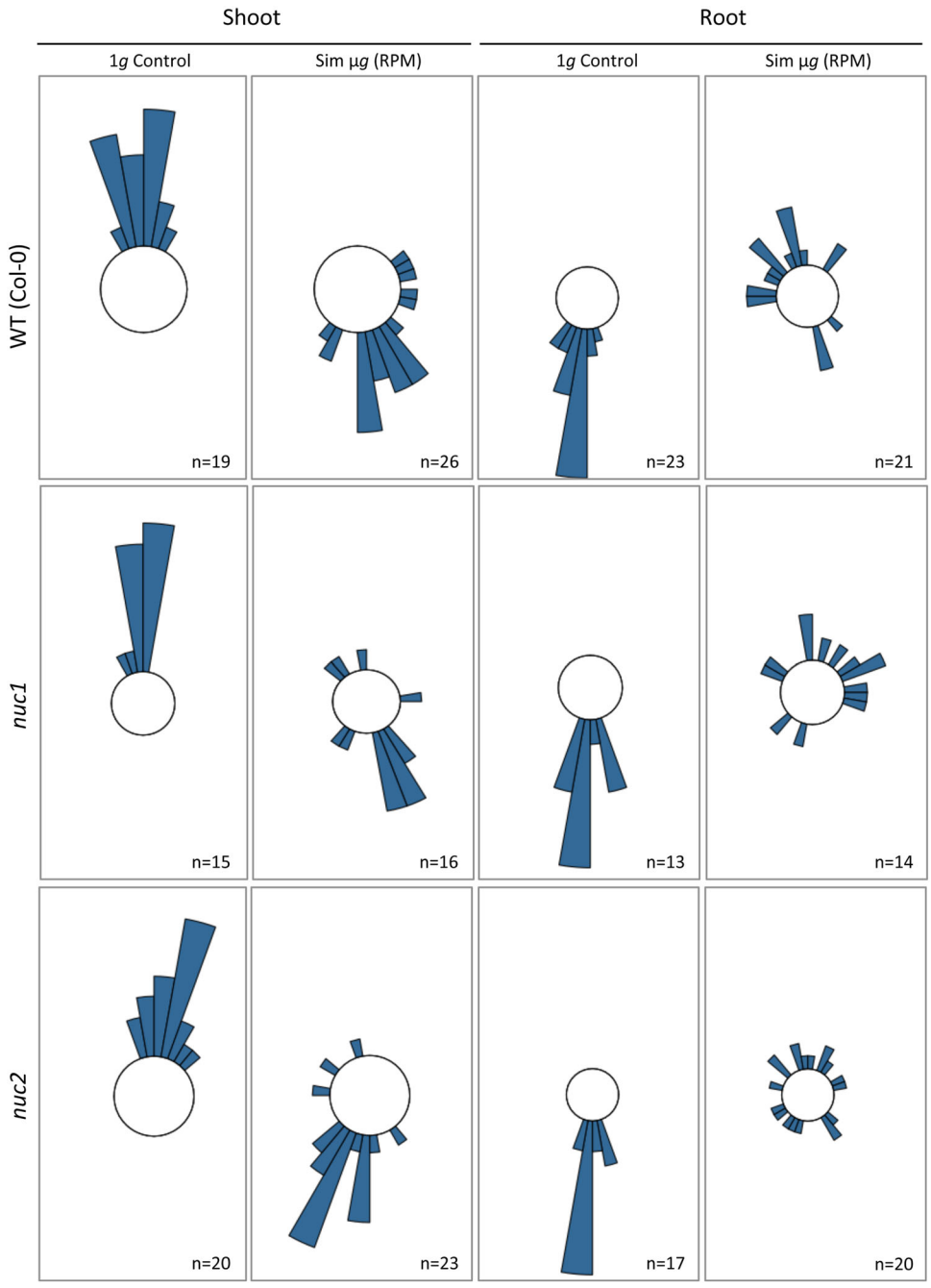

FIGURE 2 Quantification of growth orientation in hypocotyls (left) and roots (right) of dark-grown seedlings. Growth angle in 6-day-old seedlings (Col-0, mutants *nuc1* and *nuc2*) grown in darkness under simulated microgravity and in the ground gravity control condition (1 *g*) was measured. Frequencies of hypocotyl and root tip growth directions (angles) are shown in the corresponding angular position around a circle at intervals of 10° ($n = 13–26$). The angles relative to the vertical axis were measured from digital images using ImageJ software. Sample sizes are in lower right corners

condition (1 *g*) (Figure 4B, C). Quantification of the ratios between band intensity and of the 25 S to 18 S rRNA ratio using ImageJ did not reveal differences between conditions (Appendices S8–S11).

Pre-rRNA processing in the root

Root biomass in *Arabidopsis* seedlings is lower than hypocotyl biomass. Therefore, the amount of RNA that we could extract from the root is a constraint for the analytical methods potentially usable. Due to this constraint, a slightly different approach was used to detect alterations in ribosome biogenesis in the root.

The efficiency of primary transcript processing (45 S pre-rRNA) in roots was analyzed by RNA quantification at both ends of the transcript (5′ETS and 3′ETS) and by quantification of 25 S rRNA by RT-qPCR (Figure 5A). Quantification of external RNA sequences of the primary transcript could serve to detect alterations in early

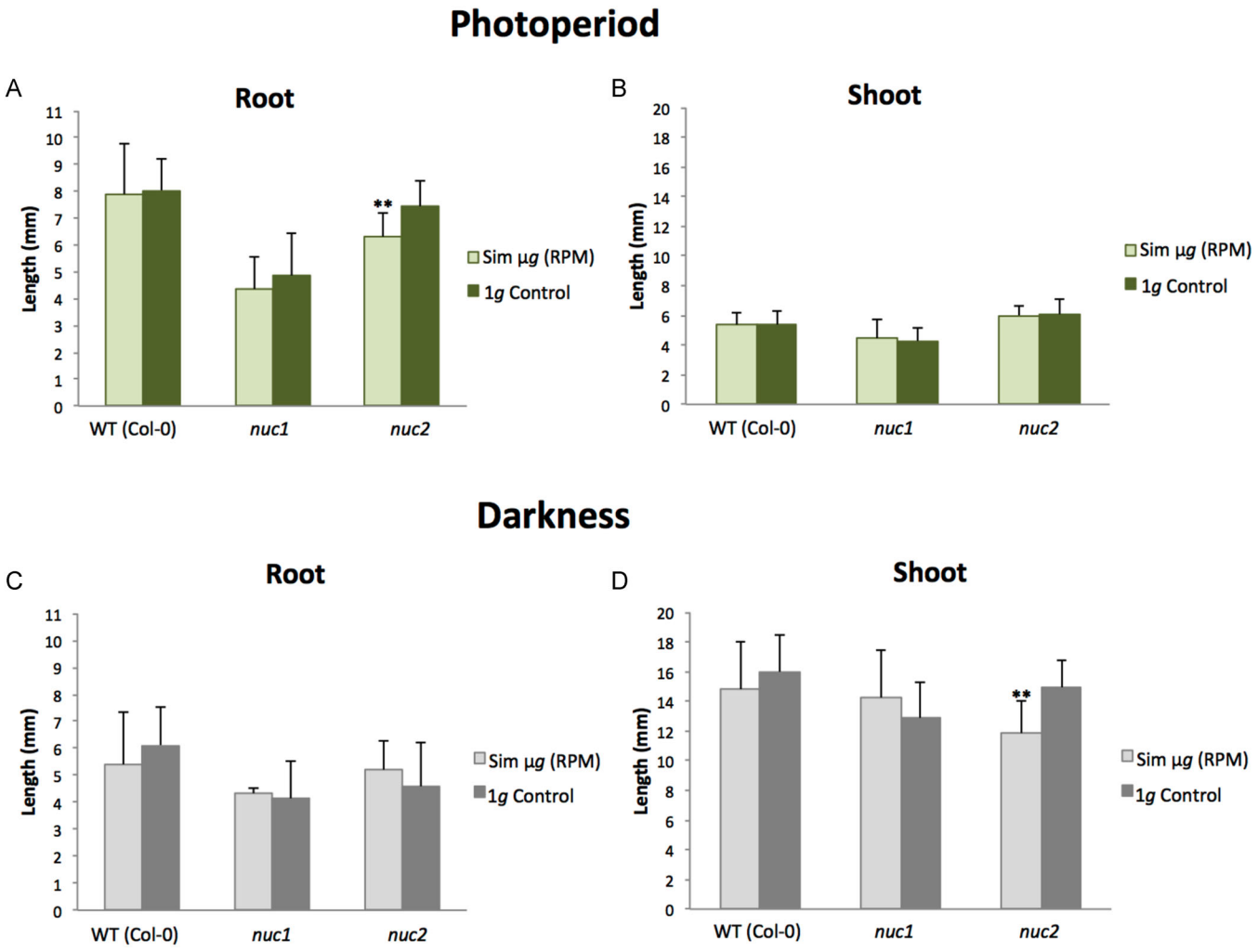

FIGURE 3 Length of root (B, D) and shoot (A, C) in seedlings grown at simulated microgravity under a photoperiod regime (A, B) or in darkness (C, D). Bars indicate standard deviation. Asterisks (**) indicate a significant difference ($P < 0.0125$) between samples of the same genotype in different gravity conditions

pre-rRNA processing, whereas different levels of 25 S rRNA would indicate a general alteration of ribosome biosynthesis (Sáez-Vásquez et al., 2004; Comella et al., 2008).

When the seedlings grew in the RPM (Sim µg) with photoperiod regime, more 25 S rRNA accumulated in all genotypes (Col-0, *nuc1*, and *nuc2*). However, sequences at both ends of the primary transcript (5′ETS and 3′ETS) only accumulated in Col-0 and the *nuc2* mutant, but they appeared to be lower in *nuc1* mutant. Comparisons were always done with respect to 1 *g* control (Figure 5B and Appendix S6).

On the other hand, in seedlings subjected to microgravity without light, the ETS pre-rRNA accumulation was different for the two ends. For 5′ETS, ETS pre-rRNA was higher in wild type (Col-0), but lower in the *nuc1* mutant, whereas the 3′ETS extreme was lower in the two mutant lines (*nuc1* and *nuc2*) than in their corresponding 1 *g* controls. The simulated microgravity exposure leads to greater 25 S rRNA accumulation in the *nuc2* mutant ($P < 0.05$), but lower accumulation in the *nuc1* mutant ($P < 0.0125$) than in the 1 *g* control condition. (Figure 5C; Appendix S6).

Factors of meristematic competence: microscopical analyses in the root tip

Cell proliferation: number of cells/mm

The rate of local cell production (LCPR, number of cells/mm in cell rows) is a variable indicative of cell proliferation activity (Scheres et al., 2002). This variable was measured in root meristematic cell layers, identified in a central optical section from the *z*-stack obtained with a confocal laser microscope, after root staining with the "Renaissance" dye for selective visualization of the cell wall (Musielak et al., 2015).

Simulated microgravity (RPM) along with photoperiod regime had no effect on this variable, since no statistically significant differences between microgravity samples and 1 *g* control samples were observed (Figure 6A). Instead, in darkness and simulated microgravity, this variable weakly decreased with respect to the control in wild type and *nuc2* plants, and the decrease was statistically significant in the least restrictive analyses ($P < 0.05$) only in *nuc1* mutant (Figure 6B; Appendix S6).

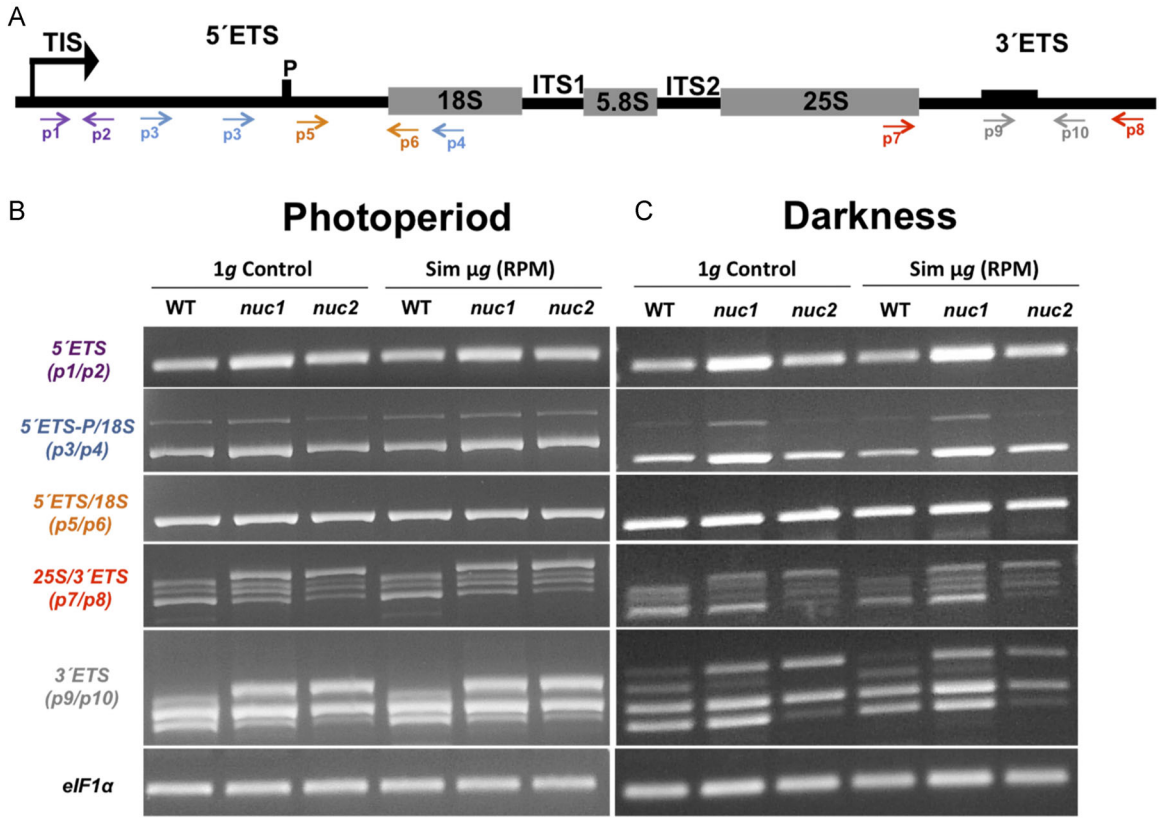

FIGURE 4 Ribosome biogenesis study in aerial part (hypocotyl) of *Arabidopsis thaliana* seedlings (Col-0, mutants *nuc1* and *nuc2*) grown under simulated microgravity and ground gravity by RT-PCR. (A) Scheme of 45 S pre-rRNA indicating amplification sequences for each primer pair, 5′ETS (p1/p2), 5′ETS-P/18 S (p3/p4); 5′ETS/18 S (p5/p6), 25 S/3′ETS (p7/p8), and 3′ETS (p9/p10). Agarose gel images of seedlings grown with photoperiod regime (B) or in darkness (C). The images shown in (B) and (C) were cropped from the originals in Appendix S12 and S13, respectively

Cyclin B1 expression

Cyclin B1 gene expression is an indicator of cell proliferation activity due to its regulator role in the G2/M cell cycle transition checkpoint (Colon-Carmona et al., 1999). The use of the CYCB1:*uid*A reporter line allowed the estimation of the expression of this gene by GUS staining, whose intensity was quantified in root meristems by measuring the integrated optical density (IOD).

In samples grown under the photoperiod, the expression of this gene was apparently not affected by the level of gravity, since no quantitatively significant differences were evident between samples grown in simulated microgravity and those grown in the 1 *g* control (Figure 6C). In general, we noticed that GUS staining corresponding to the expression of the cyclin B1 gene was rather weak in all cases.

However, GUS staining was especially weak in seedlings grown for 6 days in darkness, whatever the level of gravity, most likely due to the low availability of sugars in conditions preventing photosynthesis to be performed. In these samples, staining intensity was 10 times lower than in samples grown under a photoperiod regime, and staining intensity did not differ between the gravity levels (not shown).

Cell growth: nucleolar area

Nucleolar size is closely correlated with the rate of ribosome biogenesis and hence with cell growth in actively proliferating meristematic cells (Baserga, 2007; Bernstein et al., 2007). Nucleolar size was estimated based on the area immunostained by anti-fibrillarin antibody in the root meristematic cell layers from a central optical section.

Nucleolar size was not significantly altered in the comparison of seedlings grown in simulated microgravity (RPM) and ground control (1 *g*) when they were grown under a photoperiod regime (Figure 7A). On the contrary, the simulated microgravity and darkness clearly decreased nucleolar size/cell growth in all *Arabidopsis thaliana* lines in comparison with the 1 *g* control. This decrease was only significant for the *nuc1* and *nuc2* mutants (Figure 7B; Appendix S6).

Auxin distribution pattern

The DII-VENUS transgenic reporter line was used to compare auxin distribution in the distal part of the root under simulated microgravity for the two light conditions

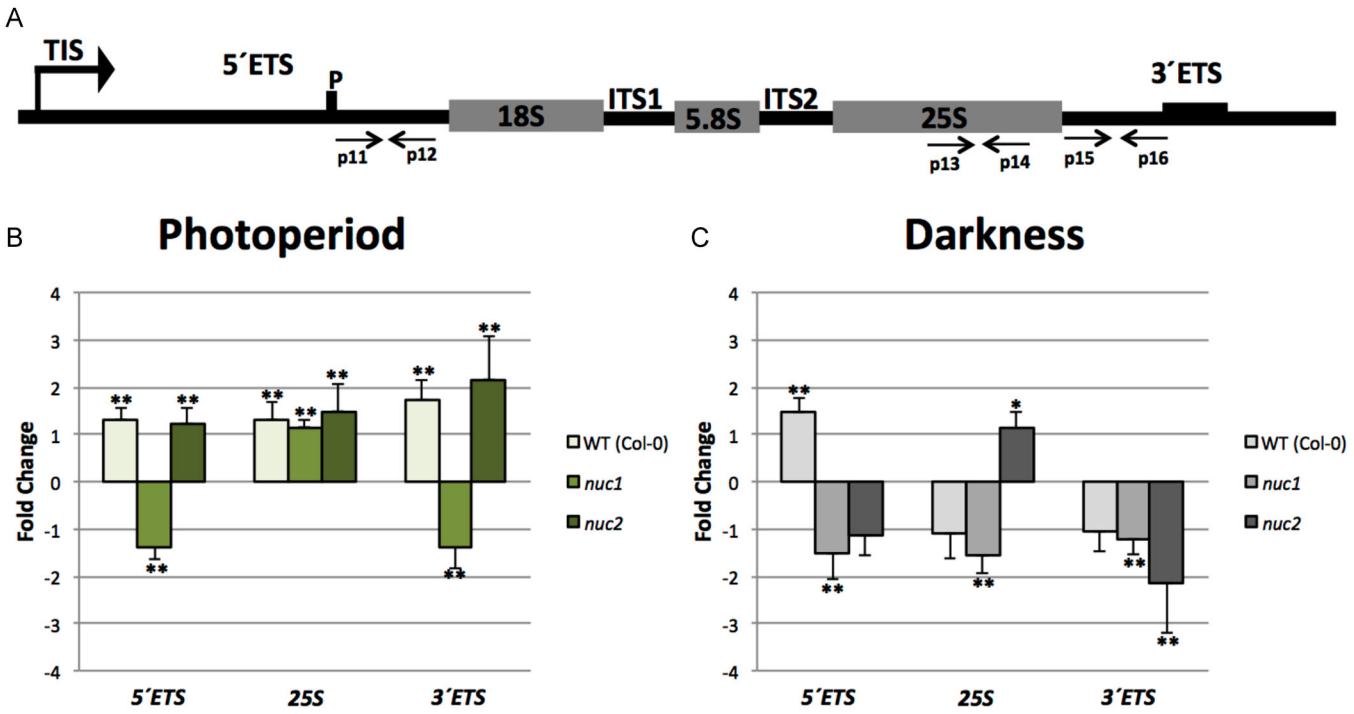

FIGURE 5 Analysis of primary transcript (45 S pre-rRNA) in roots of 6-day-old *Arabidopsis thaliana* seedlings (Col-0, mutants *nuc1* and *nuc2*) by RT-qPCR. (A) Scheme of 45 S pre-rRNA indicating amplification sequences for each primers pair, 5′ETS (p11/p12), 25 S (p13/p14) and 3′ETS (p15/p16). Relative amplification (fold-change) under simulated microgravity (RPM) respect to the ground-gravity (1*g*) control of 5′ETS and 3′ETS ends and 25 S RNA. (B) Seedlings grown with photoperiod regime. (C) Seedlings grown in absence of light (darkness). Bars indicate standard deviation. Significant differences for each genotype compared to their corresponding 1*g* control are shown (*$P < 0.05$, **$P < 0.0125$) (three biological replicates)

with that in the 1 *g* control. The reporter gene of the DII-VENUS line is a YFP construction in phase with the DII domain of the Aux/IAA protein and a nucleus location sequence. The degradation of the fusion protein is catalyzed by the $SCF^{TIR/AFB1-5}$ ubiquitination complex in the presence of auxin. Consequently, the fluorescence signal intensity in the cell nucleus when using this transgenic line is inversely proportional to the auxin level (Brunoud et al., 2012).

The fluorescence distribution in seedlings subjected to simulated microgravity and the photoperiod regime was essentially similar to that in the control seedlings grown at 1 *g*; no lateral imbalance or alteration of auxin distribution in the root was observed (Figure 8A, B). In samples grown in simulated microgravity and darkness, however, signal intensity was lower in the meristematic cell layers, central cylinder and columella cells than in the 1 *g* control, indicating that the lack of gravity stimulus alters the auxin distribution in the root. More auxin is accumulated in the distal part of the root, indicating that the transport of this phytohormone is altered, or even inhibited (Figure 8A, B). In general, the intensity of labeling was higher in the samples grown with photoperiod than in samples grown in darkness (Figure 8A, B). Thus, whatever the gravity conditions, culture in darkness alone induces some accumulation of auxin in the root tip, which appears increased in simulated microgravity.

Factors of meristematic competence: molecular biology analysis

In addition to the cellular analysis of the factors of meristematic competence, we used a complementary approach to the same biological functions (cell proliferation, cell growth, and auxin polar transport) by means of a transcriptomic (RT-qPCR) study with RNA extracted from roots.

The analysis investigated, in the conditions of gravity and light used throughout this paper, expression changes in three sets of marker genes. The first set was composed of two genes involved in auxin polar transport (*EIR/PIN2*) and auxin perception (*TIR*); the second set was composed of genes to indicate cell proliferation status because they are involved in cell cycle regulation (*CYCB1;2* and *CK2A;2*); the third set was composed of genes involved in regulating ribosome biogenesis (*NUC1*, *NUC2,* and *FIB*), hence, indicators of cell growth status.

The analysis of the relative expression of these genes (fold-change) in seedlings of the three lines grown under simulated microgravity (RPM) and photoperiod regime compared with expression in the 1 *g* controls showed that the gravity alteration produces a general down-regulation, differently affecting the concerned functions and the different lines. Auxin polar transport was

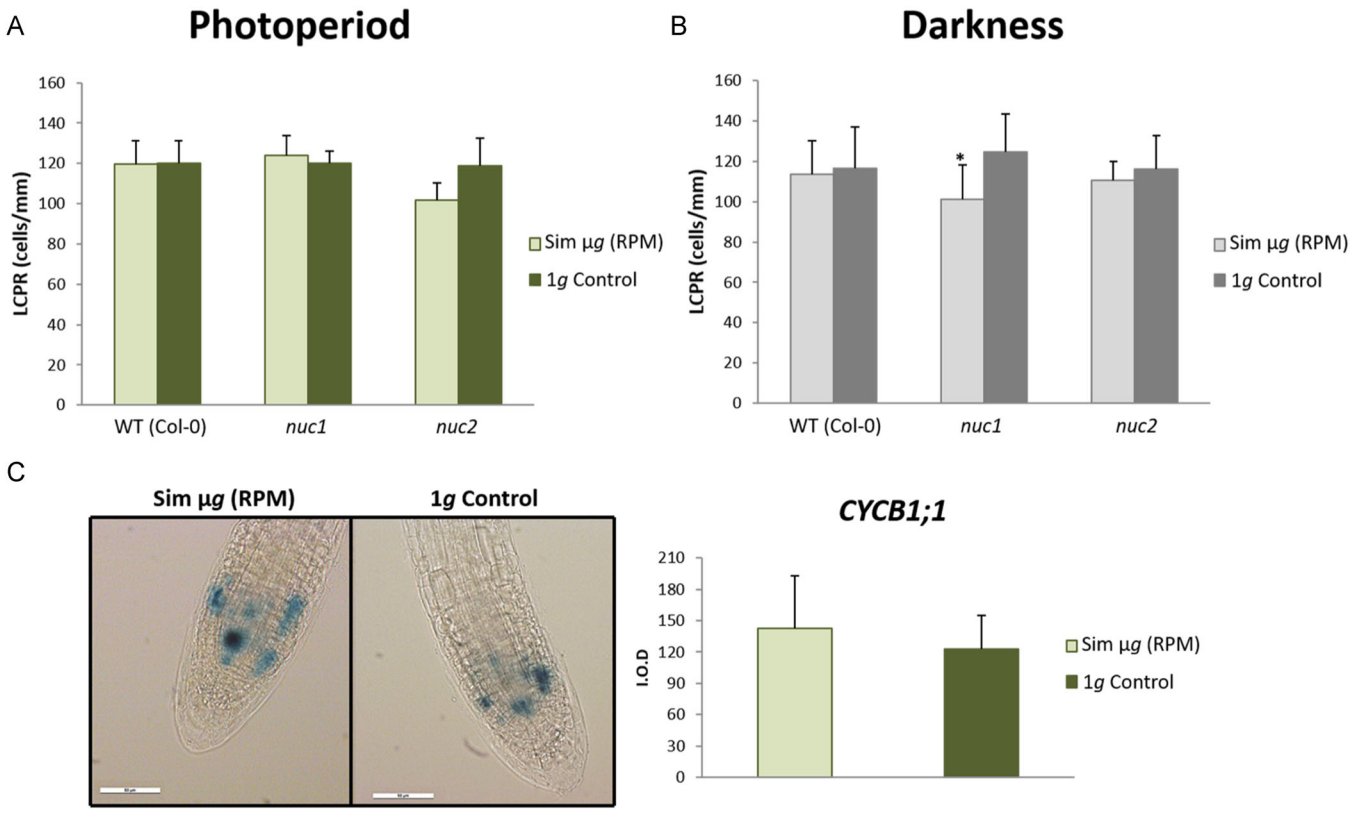

FIGURE 6 Cell proliferation rate in root meristematic cells of seedlings grown under simulated microgravity (RPM) and ground-gravity (1*g*) control conditions with photoperiod regime (A) and in darkness (B). Cyclin B1 expression in root meristem determined by the GUS signal in a reporter line. An example of a root tip is provided for simulated microgravity and 1*g* control conditions under photoperiod regime (C). In the graph, the cyclin B1 signal has been quantified as the optical density (I.O.D.). Bars indicate standard deviation. Asterisks (*) indicate a significant difference ($P < 0.05$, Student's *t*-test) between samples of the same genotype in different gravity conditions

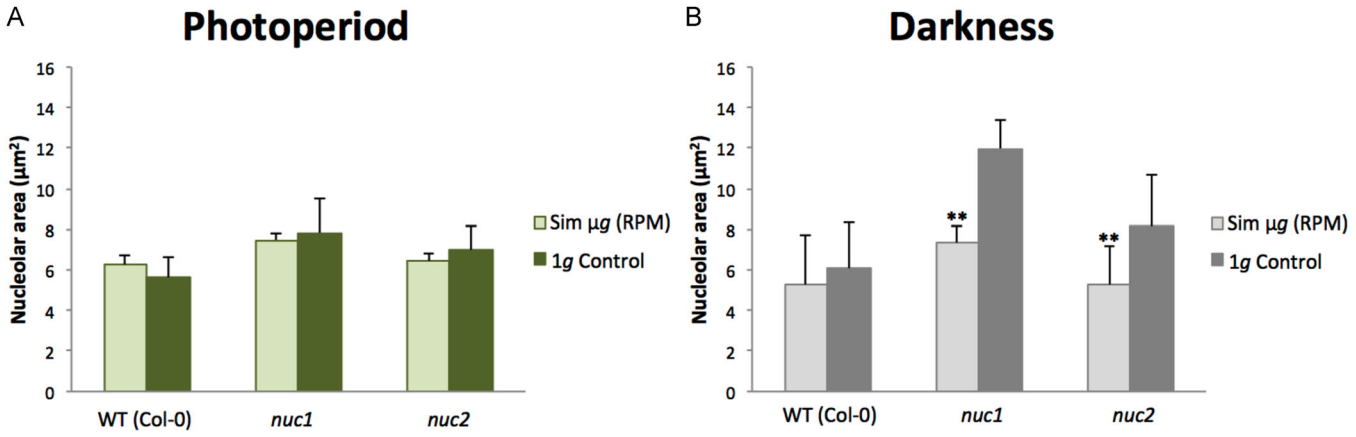

FIGURE 7 Cell growth rate (average size of the nucleolus determined by immunohistological detection of fibrillarin) under simulated microgravity and the ground-gravity (1*g*) control for seedlings grown for 6 days with photoperiod (A) or in dark conditions (B). Bars indicate standard deviation. Asterisks (**) indicate a significant difference ($P < 0.0125$) between samples of the same genotype in different gravity conditions

altered, as indicated by the decrease of *EIR* gene expression in all lines. Also, in *nuc1* mutant, expression of the auxin receptor gene *TIR* greatly decreased (Figure 9A and Appendix S6). The expression of *CYCB1;2* also markedly decreased in simulated microgravity conditions in the wild-type Col-0 and in both mutant lines (*nuc1* and *nuc2*). In contrast, *CK2A;2* expression significantly decreased only in the *nuc1* mutant (Figure 8A; Appendix S6). In turn, changes in the expression of the cell growth markers were less clear. Only the decreased expression of the *NUC2* gene in the *nuc1* mutant and increased expression of the *FIB* gene in the *nuc2* mutant differed

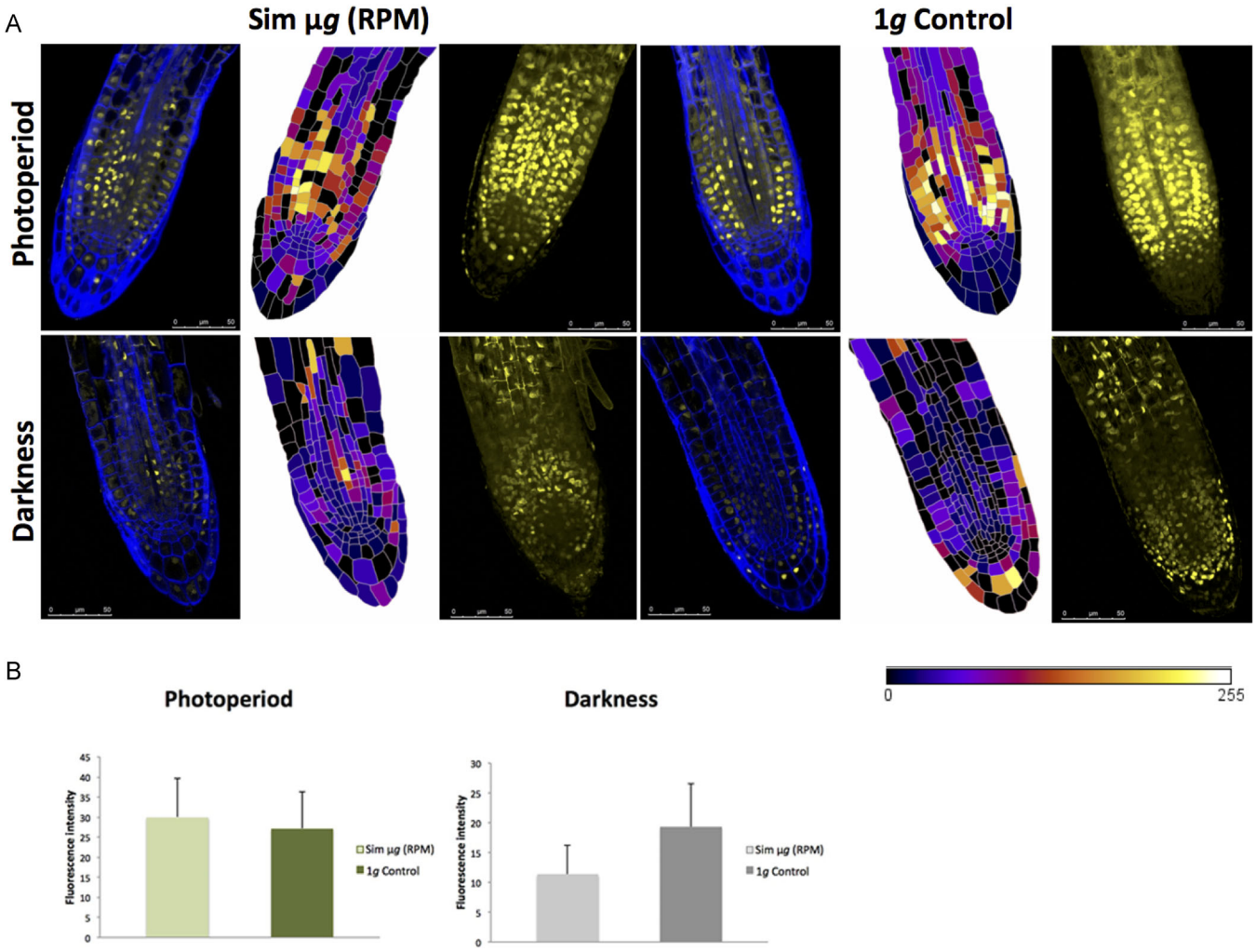

FIGURE 8 (A) Auxin distribution pattern in root tips of DII-VENUS seedlings grown for 6 days under simulated microgravity (RPM, left) or ground-gravity (1*g*) condition (right), and with photoperiod regime (first row), or in dark condition (second row). Three views per condition are shown: in the first, the yellow fluorescence signal corresponds to YFP VENUS protein, and blue fluorescence signal corresponds to the cell membrane staining with Renaissance dye; the second view shows a graphic quantification of auxin distribution, by applying a virtual color scale to the fluorescence signal intensity, from black (0) to white (255, maximum signal), using only central confocal sections of the root; the third and last view of each sample shows the confocal microscope maximum projection of the yellow fluorescence signal. The color scale is represented in the figure. (B) Quantification of the absence of auxin (mean yellow fluorescence reporter DII-VENUS) in 6-day-old plants grown under simulated microgravity (RPM) and in the 1 *g* control condition with a photoperiod lighting regime (A) or in darkness (B). The quantification corresponds to yellow fluorescence signal of the maximum projection. Bars indicate standard deviation

significantly from the controls, while no alteration of any of these markers was produced in Col-0 (Figure 9A and Appendix S6).

The results in the dark conditions showed, in general, the opposite trend. The auxin transport markers were altered in simulated microgravity and darkness, as shown by the increase in *TIR* gene expression in Col-0 and the two mutants. Expression of *EIR* increased only in the *nuc2* mutant ($P < 0.05$) (Figure 9B and Appendix S6). In the case of cell proliferation markers, the *CYCB1;2* gene decreased in expression in the *nuc1* mutant, but increased in the *nuc2* mutant, whereas the expression of *CK2A;2* gene appeared only increased in Col-0 plants (Figure 9B; Appendix S6). The expression of all cell growth markers (*NUC1*, *NUC2*, and *FIB*) was upregulated in wild-type (Col-0) seedlings compared to the 1 *g* control, whereas only *FIB* expression was upregulated significantly ($P < 0.05$) in the *nuc2* mutant (Figure 9B; Appendix S6).

DISCUSSION

The *Arabidopsis thaliana* seedlings of three different genetic backgrounds (Col-0, mutant *nuc1* and *nuc2*) grown under simulated microgravity (Sim µg, RPM) with a photoperiod regime had oriented hypocotyls and roots, the same as in the 1 *g* control samples. In other words, because the hypocotyls presented positive phototropism and the roots negative phototropism, and the phototropic axis coincided with the gravitropic axis, phototropism by itself was able to drive seedling growth in the absence of a gravitropic signal. However, plants in the absence of any tropistic signal to

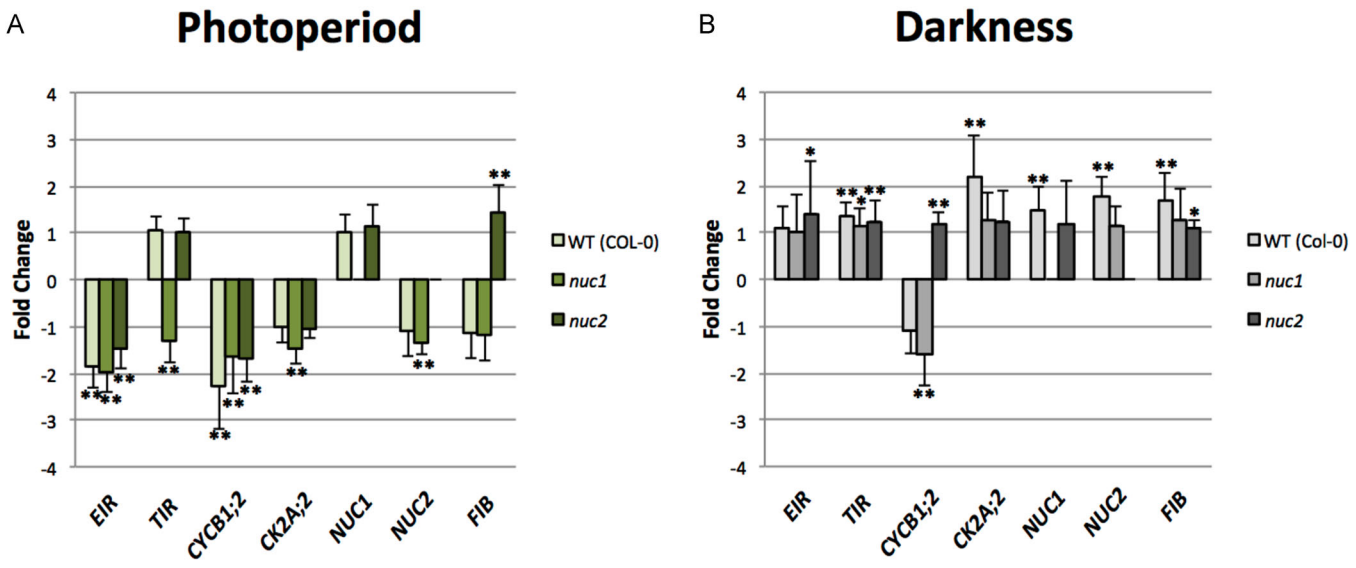

FIGURE 9 Relative expression of marker genes of auxin transport/perception, cell proliferation, and cell growth in *Arabidopsis thaliana* seedlings (Col-0, mutants *nuc1* and *nuc2*) grown under simulated microgravity with photoperiod regime (A) or darkness (B) for 6 days. Histograms indicate the average difference in expression (fold-change) between the microgravity samples versus the ground-gravity (1*g*) control samples, calculated in three biological replicates. Significant differences for each genotype respect to their corresponding 1*g* control are shown (*$P < 0.05$, **$P < 0.0125$)

guide their growth, subjected to simulated microgravity and darkness, had disoriented hypocotyls and roots, although some anti-gravitropic growth of roots and, especially, hypocotyls, was detected after the quantification of the direction angles. However, we did not detect any preferential direction for this growth, and the growth directions never coincided with the vertical axis.

Several experiments on the International Space Station (ISS), in real microgravity, have shown that, without the gravitational cue, the position of the light source influences the growth direction of both the hypocotyl and the root. The *Arabidopsis thaliana* plants grown during an APEX01 experiment in ABRS (Advanced Biological Research System) hardware with directional light (as in our experiment) showed hypocotyls and roots with an oriented growth, the same as the corresponding Earth control. In contrast, plants grown in microgravity in Petri dishes, either exposed to environmental light, or in darkness, in the CARA (Characterizing *Arabidopsis* Root Attractions) experiment had hypocotyls and roots with a random growth direction (Ferl and Paul, 2016; Paul et al., 2017).

In addition, different studies in space revealed non-random growth directions of seedling organs, when they developed in microgravity. In an experiment during the Space Shuttle STS-95 mission, most rice roots elongated in a constant direction, forming a constant angle of about 55° relative to the axis of the caryopsis in the early phase of growth, but later the roots grew in various directions, including away from the agar (Hoson et al., 2003). In the GRAVI-1 experiment in the ISS, lentil roots initially curved strongly away from the cotyledons and then slowly straightened out, forming a relatively constant angle. This establishment of growth direction in a stimulus-free environment was termed automorphogenesis (Driss-Ecole et al., 2008). Furthermore, etiolated *A. thaliana* seedlings grown in the space shuttle exhibited a left-handed skewing response (Millar et al., 2011). Actually, the deviation of the root growth from the gravity direction, termed root skewing, has been repeatedly described (Paul et al., 2012; Roy and Bassham, 2014; Schultz et al., 2016). This root skewing has been shown to be independent of both the tropic force of gravity and the gravity-induced contact forces between roots and growth media, and, interestingly, it is more intense in the WS ecotype of *A. thaliana* than in the Col-0 ecotype. However, the molecular mechanisms underlying such growth phenomenon remain unresolved. Various genes and factors have been proposed to regulate skewing, including a complex network of processes such as polar auxin transport and cytoskeletal dynamics (Nakashima et al., 2014; Roy and Bassham, 2014). These growth patterns in *A. thaliana* have been suggested to be controlled mainly by the expression levels of two apyrases (APY1 and APY2) and by extracellular ATP concentration in a pathway involving auxin polar transport and triggered by touch stimuli resulting from the contact of the root tip with the growth medium (Yang et al., 2015). A recent study in the ISS, using two mutants for skewing behavior that were altered in different cellular functions, concluded that genes related to skewing could play a prominent role in plant spaceflight acclimation (Califar et al., 2020).

Interestingly, our results in simulated microgravity and different light conditions have not revealed any special orientation of roots, but an evident skewing of hypocotyls was revealed in the absence of tropistic cues (darkness and simulated microgravity). This behavior of hypocotyls has not been previously described. In general, hypocotyl skewing

has received little attention in studies of seedling growth in altered gravity.

The significant difference between the response of the root and the hypocotyl to different conditions of gravity and light is a novel finding of this work. Certainly, light is known to have a predominant effect on tropistic responses in the shoot (Molas and Kiss, 2009). Apparently, a directional light source is sufficient for the shoot to orient its growth toward this source and to develop in microgravity the same way it does in ground gravity. Experiments on the shoot apical meristem of *A. thaliana* seedlings have demonstrated that white light is able to rescue the cell cycle arrest in G1/S and G2/M transitions caused by darkness and to promote efficient ribosome biogenesis (López-Juez et al., 2008; Mohammed et al., 2018).

In particular, our study of ribosome biogenesis using markers for different steps of 45 S pre-rRNA transcript processing revealed that this process differed in its sensitivity to gravity and light between the hypocotyl and the root. In the aerial part, neither simulated microgravity nor darkness appeared to alter this process in any of the genotypes analyzed (Col-0, *nuc1*, and *nuc2*) with respect to the control in 1 *g* with the photoperiod. However, in root cells, processing of the primary pre-ribosomal transcript was affected under simulated microgravity with photoperiod regime in the wild type and *nuc2* mutant, as indicated by the higher accumulation of 5′ETS and 3′ETS ends and 25 S rRNA. These results suggest an effect on the rate of production of ribosomes. Alterations in ribosome biogenesis induced by both real and simulated microgravity in root meristematic cells and in vitro cell cultures have been reported in previous experiments from our laboratory (Matía et al., 2010; Boucheron-Dubuisson et al., 2016; Manzano et al., 2016; Kamal et al., 2018). Different indirect markers of the process were used in these studies, such as protein levels and gene expression regulation of nucleolin and fibrillarin, nucleolar proteins known to play a key regulatory role. Interestingly, in the *nuc1* mutant, simulated microgravity intensifies the defective pre-rRNA processing that occurs in this mutant under control 1 *g* gravity conditions (Pontvianne et al., 2007; Boucheron-Dubuisson et al., 2016). In the present experiment, the higher accumulation of 25 S rRNA indicates unbalanced processing of 45 S primary transcript pre-rRNA, and the lower accumulation of the intermediate 5′ETS and 3′ ETS pre-rRNA ends indicates either faster processing or lower production of 45 S precursors. However, despite these severe changes, the *nuc1* mutant is viable, not only when grown under control 1 *g* gravity conditions, but also when subjected to simulated microgravity.

Furthermore, the size and structure of the nucleolus have proven reliable markers of ribosomal biosynthetic activity. Considering that, under photoperiod, nucleolar size did not differ significantly between samples grown in simulated microgravity and samples grown under 1 *g* control gravity, then the application of photoperiod actually counteracts the alterations induced by microgravity, as well as by darkness, on this structural variable and its functional significance. In fact, the analysis of samples grown in darkness did show significant differences, especially affecting the nucleolin mutants. In a previous study, we used transmission electron microscopy to analyze the ultrastructure of the nucleolus of the *nuc1* mutant in conditions of simulated microgravity. In that case, the nucleolus appeared rather disorganized, with a loose structure in which it was difficult to identify the typical nucleolar subcomponents, and some granules were identified, corresponding to the so-called "nucleolar peri-chromatin-like granules", which are the structural expression of poor processing of pre-rRNA (Boucheron-Dubuisson et al., 2016). Thus, in this mutant, a correlation between nucleolar size and nucleolar activity cannot be established, but the increase in size is due to nucleolar disorganization and not to increased production of ribosomal precursors, as is the case in the wild type. In the wild type, previous studies in real and simulated microgravity showed that the nucleolus was reduced in size under microgravity in etiolated seedlings compared to the 1 *g* control (Matía et al., 2010; Manzano et al., 2013, 2016).

Regarding nucleolar structure, three structural types of the nucleolus have been defined based on different rates of ribosome biogenesis: vacuolated (highly active and present mainly in G2 phase of the cell cycle), compact (active and characteristic of the G1 phase), and fibrillar (inactive and present in the GO phase). Under simulated microgravity conditions, the percentage of vacuolated and compact nucleoli decreased significantly, consistently with a lower efficiency in the production and assembly of ribosome (Manzano et al., 2016; Kamal et al., 2018). The results of the present work confirm these changes and identify specific steps of the mechanism that appear modified due to the environmental change.

The status of meristematic competence has been assayed in roots of seedlings (Col-0, *nuc1*, and *nuc2*) grown under simulated microgravity and light (photoperiod) by means of the estimation of cellular variables such as number of cells per millimeter in a meristematic cell layer (rate of local cell production), cyclin B1 expression in situ, and nucleolar area based on immunolabelling of fibrillarin. Our results indicate that seedlings maintain the coordination of growth and proliferation in meristematic cells at equivalent levels to the 1 *g* control. Thus, light can compensate for microgravity stress at the cellular level. In other words, phototropism can counteract the lack of gravitropism, at least to a certain extent. These results agree with those from a clinostat experiment (Boucheron-Dubuisson et al., 2016). In general, there is increasing evidence that light is an important regulator of stress acclimation processes (Janda et al., 2020).

However, when comparing the general response to microgravity at the molecular level of the different lines (Figure 9), *nuc1* shows a differential pattern of expression of marker genes, not only for the genes affecting ribosome biogenesis, but also for genes related to auxin transport and cell cycle regulation. The alterations inherent to this mutant that reduce its efficiency in the production of ribosomes with respect to the wild type also seem to alter its response to gravitational stress in other physiological processes that

are somehow related to ribosome biogenesis and meristematic competence. Therefore, the *nuc1* mutant would have a reduced ability to counteract the lack of gravity, while the wild type and *nuc2* mutant share a common profile (but gene fold-change ratios are smaller in the case of *nuc2*). It should be noticed that the protein NUC2 is a stress-related variant of nucleolin (Durut et al., 2019). Therefore, the similar, but attenuated response to gravitational stress in this mutant could be interpreted as a sign of resilience to an adverse environmental condition.

In particular, we found expression changes in marker genes for cell proliferation and auxin transport in the root meristem. Whereas *EIR* (*PIN2*) expression decreased in the three plant genotypes (Col-0, *nuc1*, and *nuc2*), this change was not accompanied by any alteration of the auxin distribution pattern observed in the DII-VENUS line between the samples grown in microgravity and the 1 *g* control. In the space experiments CARA (with environmental light from Destiny module of ISS) and APEX03-2 (with directional light supplied by the Vegetable Production System hardware), no differences in the root meristem fluorescence pattern of pDR5r::GFP line were observed (Ferl and Paul, 2016). Therefore, the expression changes in a particular auxin transport gene (*EIR*) suggest that the process is sensitive to microgravity, but, in the presence of light, the overall efficiency of the process would not be significantly altered. The functional redundancy between PIN proteins (Swarup et al., 2001; Blilou et al., 2005; Ueda et al., 2014) could be counteracting the observed changes of gene expression.

The most severe alteration concerned the expression levels of the *CYCB1;2* gene, which showed an important decrease in simulated microgravity with respect to the 1 *g* control for the wild-type and mutants *nuc1* and *nuc2*, even under photoperiod. In real microgravity and in ground-based facilities, our laboratory has consistently found a decrease in *CYCB1* gene expression using histochemical measurements of GUS staining in *A. thaliana* reporter lines (Manzano et al., 2009; Matía et al., 2009) and RT-qPCR experiments with a cell culture exposed for 3 h to simulated microgravity. In the latter case, the observed shortening of the G2 phase of cell cycle did not produce any change in cell size between the two experimental conditions (Manzano et al., 2016). As in the present case, a molecular alteration was not correlated with any change at the cellular level.

Finally, a general question emerging from our study would be whether the differences between plants grown under microgravity conditions and under gravity conditions are independent of the effect of growing in the dark or not. The answer to this question could be better obtained with a two-factor ANOVA test than with independent analyses. Although the random assignment of treatment combinations was not fully met for this analysis, the result of the ANOVA test, which is shown in the supplementary material, shows that, for most molecular biology analyses in all three lines, interactions are significant. However, for microscopical analyses in the root tip, interactions were significant only in the mutants (Appendix S7). Therefore, the effects of light and gravity indeed depend on each other. This is an interesting conclusion, which supports previous investigations that we already mentioned (Kruse et al., 2020; Yang et al., 2020), but it corresponds to a different working hypothesis than the one that gave rise to the present work. Our purpose was to examine the counteracting role of light signals and their capability of reverting the effects of altered gravity on some variables related to cell proliferation and plant development to the standard values recorded at 1 *g*. Our results show that light signals may indeed totally or partially replace gravity signals, significantly improving plant growth and development in microgravity. The confirmation of interactions between light and gravity signals supposes an additional result, of interest in itself and also as an additional contribution to qualify the results of the work, especially from a mechanistic point of view.

CONCLUSIONS

The findings presented in this work are of great importance for successful plant culture in microgravity environments. We show indeed that light is a signal capable of rescuing disrupted meristematic competence at early developmental stages in the absence of light and gravity, the two main tropistic cues that drive and regulate plant growth on Earth. These results are decisive for long-term plant development. The incorporation of an illumination regime, in this case photoperiod, has been sufficient to attenuate or suppress the effects caused by gravitational stress, such that plants can grow and develop correctly in microgravity, showing only alterations at the molecular level but no changes detectable at the cellular level. Therefore, and as shown by other experiments carried out at real microgravity (Massa et al., 2013; De Micco et al., 2014; Link et al., 2014) and at simulated microgravity (Boucheron-Dubuisson et al., 2016; Valbuena et al., 2018), if the growth conditions are optimal (nutrients, light, temperature, humidity) the plants grow properly in their first stages of development. Despite that, molecular alterations are still compatible with the expected acclimation mechanisms involving the modulation of duplicated and specialized genes, expressed under environmental stress, such as *NUC2*, that should be promoted to increase the plant acclimation to a new extraterrestrial environment.

Therefore, to extend our knowledge on the crosstalk between these two environmental signals, future experiments should be focused on the signaling and transduction of both cues, with an emphasis on the central role of auxin in the signaling mechanisms and on answering other questions such as why auxin distribution at the root tip was not altered.

ACKNOWLEDGMENTS

This work was funded by the Agencia Estatal de Investigación of the Spanish Ministry of Science an Innovation, Grants #ESP2015-64323-R and #RTI2018-099309-B-I00 (co-funded by EU-ERDF) to F.J.M., and Bonus Recherche from the UPVD to J.S.V. The use of the facilities of microgravity simulation was provided by the ESA-CORA-Ground Based Facilities Program, contract Ref. #4000105761 to F.J.M. and

R.H. A.M. was recipient of a contract of the Program for Young Researchers Training of the Agencia Estatal de Investigación of the Spanish Ministry of Science an Innovation Ref. #BES-2013-063933. J.S.V. lab's work is set within the framework of the "Laboratoires d'Excellences (LABEX)" TULIP (ANR-10-LABX-41). Finally, we thank Dr. Guillermo Padilla, head of the Biostatistics Area of the Department of Bioinformatics and Biostatistics of CIB Margarita Salas-CSIC, for assistance with statistical analyses and interpreting the results and the reviewers and editorial group for their valuable comments that have improved the manuscript.

AUTHOR CONTRIBUTIONS

F.J.M. designed the objectives of the work and, with a major contribution from R.H., designed the experimental sequence and procedures, supervised the entire work and were the major contributors to the final version of the manuscript. A.M. performed all the experimental work, including statistics and bioinformatics, and wrote the first draft of the manuscript. V.P.L. managed the facility for microgravity simulation and assisted in the incubation of samples in this facility. J.S.V. designed and supervised the experiments involving pre-rRNA processing and provided the oligos used in these experiments. A.d.B. assisted in the experiments on pre-rRNA processing. All authors read and approved the final manuscript.

DATA AVAILABILITY STATEMENT

The data sets used and analyzed during the current study are available from from the Dryad Digital Repository: https://doi.org/10.5061/dryad.63xsj3v2 (Manzano et al., 2021).

ORCID

F. Javier Medina http://orcid.org/0000-0002-0866-7710

REFERENCES

Baserga, R. 2007. Is cell size important? *Cell Cycle* 6: 814–816.

Beemster, G. T. S., and T. I. Baskin. 1998. Analysis of cell division and elongation underlying the developmental acceleration of root growth in *Arabidopsis thaliana*. *Plant Physiology* 116: 1515–1526.

Bernstein, K. A., F. Bleichert, J. M. Bean, F. R. Cross, and S. J. Baserga. 2007. Ribosome biogenesis is sensed at the start cell cycle checkpoint. *Molecular Biology of the Cell* 18: 953–964.

Blilou, I., J. Xu, M. Wildwater, V. Willemsen, I. A. Paponov, J. Friml, R. Heidstra, et al. 2005. The PIN efflux facilitator network controls growth and patterning in *Arabidopsis* roots. *Nature* 433: 39–44.

Borst, A. G., and J. J. W. A. van Loon. 2009. Technology and developments for the Random Positioning Machine, RPM. *Microgravity Science and Technology* 21: 287–292. http://doi.org/10.1007/s12217-008-9043-2

Boucheron-Dubuisson, E., A. I. Manzano, I. Le Disquet, I. Matía, J. Sáez-Vasquez, J. J. W. A. van Loon, R. Herranz, et al. 2016. Functional alterations of root meristematic cells of *Arabidopsis thaliana* induced by a simulated microgravity environment. *Journal of Plant Physiology* 207: 30–41.

Brunoud, G., D. M. Wells, M. Oliva, A. Larrieu, V. Mirabet, A. H. Burrow, T. Beeckman, et al. 2012. A novel sensor to map auxin response and distribution at high spatio-temporal resolution. *Nature* 482: 103–106.

Caldana, C., Y. Li, A. Leisse, Y. Zhang, L. Bartholomaeus, A. R. Fernie, L. Willmitzer, and P. Giavalisco. 2013. Systemic analysis of inducible target of rapamycin mutants reveal a general metabolic switch controlling growth in *Arabidopsis thaliana*. *Plant Journal* 73: 897–909.

Califar, B., N. J. Sng, A. Zupanska, A.-L. Paul, and R. J. Ferl. 2020. Root skewing-associated genes impact the spaceflight response of *Arabidopsis thaliana*. *Frontiers in Plant Science* 11: 239.

Christie, J. M., and A. S. Murphy. 2013. Shoot phototropism in higher plants: new light through old concepts. *American Journal of Botany* 100: 35–46.

Colon-Carmona, A., R. You, T. Haimovitch-Gal, and P. Doerner. 1999. Spatio-temporal analysis of mitotic activity with a labile cyclin-GUS fusion protein. *Plant Journal* 20: 503–508. http://doi.org/10.1046/j.1365-313x.1999.00620.x

Comella, P., F. Pontvianne, S. Lahmy, F. Vignols, N. Barbezier, A. DeBures, E. Jobet, et al. 2008. Characterization of a ribonuclease III-like protein required for cleavage of the pre-rRNA in the 3'ETS in Arabidopsis. *Nucleic Acids Research* 36: 1163–1175.

De Micco, V., S. De Pascale, R. Paradiso, and G. Aronne. 2014. Microgravity effects on different stages of higher plant life cycle and completion of the seed-to-seed cycle. *Plant Biology* 16: 31–38.

Driss-Ecole, D., V. Legué, E. Carnero-Diaz, and G. Perbal. 2008. Gravisensitivity and automorphogenesis of lentil seedling roots grown on board the International Space Station. *Physiologia Plantarum* 134: 191–201.

Durut, N., M. Abou-Ellail, P. Comella, E. Jobet, A. de Bures & J. Sáez-Vásquez. 2019. NUCLEOLIN: similar and antagonistic roles in Arabidopsis thaliana. In 26th European Low Gravity Research Association Biennial Symposium and General Assembly, Book of abstracts, 150, Granada, Spain. Website: https://www.elgra.org/wp-content/uploads/2020/06/ELGRA2019-Book-of-abstracts.pdf

Durut, N., M. Abou-Ellail, F. Pontvianne, S. Das, H. Kojima, S. Ukai, A. de Bures, et al. 2014. A duplicated NUCLEOLIN gene with antagonistic activity is required for chromatin organization of silent 45S rDNA in Arabidopsis. *Plant Cell* 26: 1330–1344.

Durut, N., and J. Sáez-Vásquez. 2015. Nucleolin: dual roles in rDNA chromatin transcription. *Gene* 556: 7–12.

Ferl, R. J., and A.-L. Paul. 2016. The effect of spaceflight on the gravity-sensing auxin gradient of roots: GFP reporter gene microscopy on orbit. *npj Microgravity* 2: 15023.

Ferreira, P., A. S. Hemerly, J. De Almeida Engler, C. Bergounioux, S. Burssens, M. Van Montagu, G. Engler, and D. Inzé. 1994. Three discrete classes of Arabidopsis cyclins are expressed during different intervals of the cell cycle. *Proceedings of the National Academy of Sciences, USA* 91: 11313–11317.

Herranz, R., R. Anken, J. Boonstra, M. Braun, P. C. M. Christianen, M. de Geest, J. Hauslage, et al. 2013. Ground-based facilities for simulation of microgravity: organism-specific recommendations for their use, and recommended terminology. *Astrobiology* 13: 1–17.

Hoson, T., K. Soga, K. Wakabayashi, S. Kamisaka, and E. Tanimoto. 2003. Growth and cell wall changes in rice roots during spaceflight. *Plant and Soil* 255: 19–26.

Janda, T., É. Hideg, and R. Vanková. 2020. The role of light in abiotic stress acclimation. *Frontiers in Plant Science* 11: 184.

Kamal, K. Y., R. Herranz, J. J. W. A. van Loon, and F. J. Medina. 2018. Simulated microgravity, Mars gravity, and 2g hypergravity affect cell cycle regulation, ribosome biogenesis, and epigenetics in Arabidopsis cell cultures. *Scientific Reports* 8: 6424.

Kruse, C. P. S., A. D. Meyers, P. Basu, S. Hutchinson, D. R. Luesse, and S. E. Wyatt. 2020. Spaceflight induces novel regulatory responses in Arabidopsis seedling as revealed by combined proteomic and transcriptomic analyses. *BMC Plant Biology* 20: 237.

Link, B. M., J. S. Busse, and B. Stankovic. 2014. Seed-to-seed-to-seed growth and development of *Arabidopsis* in microgravity. *Astrobiology* 14: 866–875.

Livak, K. J., and T. D. Schmittgen. 2001. Analysis of relative gene expression data using real-time quantitative PCR and the $2^{-\Delta\Delta CT}$ method. *Methods* 25: 402–408.

López-Juez, E., E. Dillon, Z. Magyar, S. Khan, S. Hazeldine, S. M. de Jager, J. A. H. Murray, et al. 2008. Distinct light-initiated gene expression and cell cycle programs in the shoot apex and cotyledons of *Arabidopsis*. *Plant Cell* 20: 947–968.

Manzano A. I., R. Herranz, A. Manzano, and J. J. W. A. van Loon. 2016. Early effects of altered gravity environments on plant cell growth and cell

proliferation: characterization of morphofunctional nucleolar types in an *Arabidopsis* cell culture system. *Frontiers in Astronomy and Space Sciences* 3. http://doi.org/10.3389/fspas.2016.00002

Manzano, A. I., O. Larkin, C. Dijkstra, P. Anthony, M. Davey, L. Eaves, R. Hill, et al. 2013. Meristematic cell proliferation and ribosome biogenesis are decoupled in diamagnetically levitated *Arabidopsis* seedlings. *BMC Plant Biology* 13: 124.

Manzano, A. I., I. Matía, F. González-Camacho, E. Carnero-Diaz, J. J. W. A. van Loon, C. Dijkstra, O. Larkin, P. Anthony, M. R. Davey, R. Marco, and F. J. Medina. 2009. Germination of Arabidopsis seed in space and in simulated microgravity: alterations in root cell growth and proliferation. *Microgravity Science and Technology* 21: 293–297.

Manzano, A., A. Villacampa, J. Sáez-Vásquez, J. Z. Kiss, F. J. Medina, and R. Herranz. 2020. The importance of Earth reference controls in spaceflight -omics research: characterization of nucleolin mutants from the seedling growth experiments. *iScience* 23: 101686.

Manzano, A., V. Pereda-Loth, A. de Bures, J. Sáez-Vásquez, R. Herranz, and F. J. Medina. 2021. Data from: Light signals counteract alterations caused by simulated microgravity in proliferating plant cells. *Dryad Digital Repository*. https://doi.org/10.5061/dryad.63xsj3v2

Massa, G. D., G. Newsham, M. E. Hummerick, J. L. Caro, G. W. Stutte, R. C. Morrow, and R. M. Wheeler. 2013. Preliminary species and media selection for the Veggie space hardware. *Gravitational and Space Research* 1: 95–106.

Matía, I., F. González-Camacho, R. Herranz, J. Z. Kiss, G. Gasset, J. J. W. A. van Loon, R. Marco, and F. J. Medina. 2010. Plant cell proliferation and growth are altered by microgravity conditions in spaceflight. *Journal of Plant Physiology* 167: 184–193.

Matía, I., J. W. A. van Loon, E. Carnero-Diaz, R. Marco, and F. J. Medina. 2009. Seed germination and seedling growth under simulated microgravity causes alterations in plant cell proliferation and ribosome biogenesis. *Microgravity Science and Technology* 21: 169–174.

Medina, F. J., A. Cerdido, and G. De Cárcer. 2000. The functional organization of the nucleolus in proliferating plant cells. *European Journal of Histochemistry* 44: 117–131.

Medina, F. J., F. González-Camacho, A. I. Manzano, A. Manrique, and R. Herranz. 2010. Nucleolin, a major conserved multifunctional nucleolar phosphoprotein of proliferating cells. *Journal of Applied Biomedicine* 8: 141–150.

Millar, K. D., C. M. Johnson, R. E. Edelmann, and J. Z. Kiss. 2011. An endogenous growth pattern of roots is revealed in seedlings grown in microgravity. *Astrobiology* 11: 787–797.

Mizukami, Y. 2001. A matter of size: developmental control of organ size in plants. *Current Opinion in Plant Biology* 4: 533–539.

Mohammed, B., S. F. Bilooei, R. Dóczi, E. Grove, S. Railo, K. Palme, F. A. Ditengou, et al. 2018. Converging light, energy and hormonal signaling control meristem activity, leaf initiation, and growth. *Plant Physiology* 176: 1365–1381.

Molas, M. L., and J. Z. Kiss. 2009. Phototropism and gravitropism in plants. *Advances in Botanical Research* 49: 1–34.

Mongelard, F., and P. Bouvet. 2007. Nucleolin: a multiFACeTed protein. *Trends in Cell Biology* 17: 80–86.

Musielak, T. J., L. Schenkel, M. Kolb, A. Henschen, and M. Bayer. 2015. A simple and versatile cell wall staining protocol to study plant reproduction. *Plant Reproduction* 28: 161–169.

Nakashima, J., F. Liao, J. A. Sparks, Y. Tang, and E. B. Blancaflor. 2014. The actin cytoskeleton is a suppressor of the endogenous skewing behaviour of *Arabidopsis* primary roots in microgravity. *Plant Biology* 16: 142–150.

Ottenschlager, I., P. Wolff, C. Wolverton, R. P. Bhalerao, G. Sandberg, H. Ishikawa, M. Evans, and K. Palme. 2003. Gravity-regulated differential auxin transport from columella to lateral root cap cells. *Proceedings of the National Academy of Sciences, USA* 100: 2987–2991.

Paul, A.-L., C. Amalfitano, and R. Ferl. 2012. Plant growth strategies are remodeled by spaceflight. *BMC Plant Biology* 12: 232.

Paul, A.-L., N. J. Sng, A. K. Zupanska, A. Krishnamurthy, E. R. Schultz, and R. J. Ferl. 2017. Genetic dissection of the Arabidopsis spaceflight transcriptome: Are some responses dispensable for the physiological adaptation of plants to spaceflight? *PLoS One* 12: e0180186.

Perrot-Rechenmann, C. 2010. Cellular responses to auxin: division versus expansion. *Cold Spring Harbor Perspectives in Biology* 2: a001446.

Pontvianne, F., M. Abou-Ellail, J. Douet, P. Comella, I. Matia, C. Chandrasekhara, A. DeBures, et al. 2010. Nucleolin is required for DNA methylation state and the expression of rRNA gene variants in *Arabidopsis thaliana*. *PLoS Genetics* 6: e1001225.

Pontvianne, F., I. Matía, J. Douet, S. Tourmente, F. J. Medina, M. Echeverría, and J. Sáez-Vasquez. 2007. Characterization of *AtNUC-L1* reveals a central role of nucleolin in nucleolus organization and silencing of *AtNUC-L2* gene in *Arabidopsis*. *Molecular Biology of the Cell* 18: 369–379.

Pound, M. P., A. P. French, D. M. Wells, M. J. Bennett, and T. P. Pridmore. 2012. CellSeT: novel software to extract and analyze structured networks of plant cells from confocal images. *Plant Cell* 24: 1353–1361.

Roy, R., and D. C. Bassham. 2014. Root growth movements: waving and skewing. *Plant Science* 221–222: 42–47.

Sablowski, R., and M. Carnier Dornelas. 2014. Interplay between cell growth and cell cycle in plants. *Journal of Experimental Botany* 65: 2703–2714.

Sáez-Vásquez, J., D. Caparros-Ruiz, F. Barneche, and M. Echeverría. 2004. A plant snoRNP complex containing snoRNAs, fibrillarin, and nucleolin-like proteins is competent for both rRNA gene binding and pre-rRNA processing in vitro. *Molecular and Cellular Biology* 24: 7284–7297.

Sáez-Vásquez, J., and F. J. Medina. 2008. The plant nucleolus. *In* J. C. Kader and M. Delseny [eds.], Advances in botanical research Vol. 47, 1–46. Elsevier, San Diego, CA, USA.

Scheres, B., P. Benfey, and L. Dolan. 2002. Root development. *The Arabidopsis book* 1: e0101. http://doi.org/10.1199/tab.0101

Schultz, E. R., A.-L. Paul, and R. J. Ferl. 2016. Root growth patterns and morphometric change based on the growth media. *Microgravity Science and Technology* 28: 621–631.

Silva-Navas, J., M. A. Moreno-Risueño, C. Manzano, B. Téllez-Robledo, S. Navarro-Neila, V. Carrasco, S. Pollmann, et al. 2016. Flavonols mediate root phototropism and growth through regulation of proliferation-to-differentiation transition. *Plant Cell* 28: 1372–1387.

Swarup, R., J. Friml, A. Marchant, K. Ljung, G. Sandberg, K. Palme, and M. Bennett. 2001. Localization of the auxin permease AUX1 suggests two functionally distinct hormone transport pathways operate in the Arabidopsis root apex. *Genes & Development* 15: 2648–2653.

Ueda, J., K. Miyamoto, E. Uheda, M. Oka, S. Yano, A. Higashibata, and N. Ishioka. 2014. Close relationships between polar auxin transport and graviresponse in plants. *Plant Biology* 16: 43–49.

Valbuena, M. A., A. Manzano, J. P. Vandenbrink, V. Pereda-Loth, E. Carnero-Diaz, R. E. Edelmann, J. Z. Kiss, et al. 2018. The combined effects of real or simulated microgravity and red-light photoactivation on plant root meristematic cells. *Planta* 248: 691–704.

Vandenbrink, J. P., J. Z. Kiss, R. Herranz, and F. J. Medina. 2014. Light and gravity signals synergize in modulating plant development. *Frontiers in Plant Science* 5: 563.

Weis, B. L., J. Kovacevic, S. Missbach, and E. Schleiff. 2015. Plant-specific features of ribosome biogenesis. *Trends in Plant Science* 20: 729–740.

Xiong, Y., M. McCormack, L. Li, Q. Hall, C. Xiang, and J. Sheen. 2013. Glucose-TOR signalling reprograms the transcriptome and activates meristems. *Nature* 496: 181–186.

Yang, P., Q. Wen, R. Yu, X. Han, X. W. Deng, and H. Chen. 2020. Light modulates the gravitropic responses through organ-specific PIFs and HY5 regulation of *LAZY4* expression in *Arabidopsis*. *Proceedings of the National Academy of Sciences, USA* 117: 18840–18848.

Yang, X., B. Wang, B. Farris, G. Clark, and S. J. Roux. 2015. Modulation of root skewing in Arabidopsis by apyrases and extracellular ATP. *Plant and Cell Physiology* 56: 2197–2206.

SUPPORTING INFORMATION

Additional supporting information may be found online in the Supporting Information tab for this article.

Appendix S1. Desktop RPM facility inside incubator and $1 \times g$ control scaffold.
Appendix S2. Primer sequences used for pre-RNA 45S processing study in aerial part (hypocotyl) of plants.
Appendix S3. RT-qPCR primer sequences.
Appendix S4. Melting curves for primers used in the RT-qPCR.
Appendix S5. Expression levels of genes or pre-rRNA analyzed in each of the experimental conditions.
Appendix S6. Statistical report.
Appendix S7. Two-way ANOVA analyses.
Appendix S8. RT-PCR of pre-rRNA processing in aerial part (hypocotyl) of *Arabidopsis thaliana* seedlings grown with photoperiod regime.
Appendix S9. RT-PCR of pre-rRNA processing in aerial part (hypocotyl) of *Arabidopsis thaliana* seedlings (Col-0, mutants *nuc1* and *nuc2*) grown without light.
Appendix S10. 25S/18S RNA ratio in total RNA in aerial part (hypocotyl) of seedlings grown under photoperiod regime.
Appendix S11. 25S/18S RNA ratio in total RNA in aerial part (hypocotyl) of seedlings grown without light.
Appendices S12–S15. Original uncropped agarose gels.

How to cite this article: Manzano, A., V. Pereda-Loth, A. de Bures, J. Sáez-Vásquez, R. Herranz, and F. J. Medina. 2021. Light signals counteract alterations caused by simulated microgravity in proliferating plant cells. *American Journal of Botany* 108(9): 1–18. https://doi.org/10.1002/ajb2.1728